

***Arabidopsis* PHYTOCHROME INTERACTING FACTOR Proteins Promote Phytochrome B Polyubiquitination by COP1 E3 Ligase in the Nucleus**

In-Cheol Jang,^a Rossana Henriques,^a Hak Soo Seo,^{a,1} Akira Nagatani,^b and Nam-Hai Chua^{a,2}

^aLaboratory of Plant Molecular Biology, The Rockefeller University, New York, New York 10065

^bDepartment of Botany, Graduate School of Science, Kyoto University, Kitashirakawa, Kyoto 606-8502, Japan

Many plant photoresponses from germination to shade avoidance are mediated by phytochrome B (phyB). In darkness, phyB exists as the inactive Pr in the cytosol but upon red (R) light treatment, the active Pfr translocates into nuclei to initiate signaling. Degradation of phyB Pfr likely regulates signal termination, but the mechanism is not understood. Here, we show that phyB is stable in darkness, but in R, a fraction of phyB translocates into nuclei and becomes degraded by 26S proteasomes. Nuclear phyB degradation is mediated by COP1 E3 ligase, which preferentially interacts with the PhyB N-terminal region (PhyB-N). PhyB-N polyubiquitination by CONSTITUTIVE PHOTOMORPHOGENIC1 (COP1) *in vitro* can be enhanced by different PHYTOCHROME INTERACTING FACTOR (PIF) proteins that promote COP1/PhyB interaction. Consistent with these results, nuclear phyB accumulates to higher levels in *pif* single and double mutants and in *cop1-4*. Our results identify COP1 as an E3 ligase for phyB and other stable phytochromes and uncover the mechanism by which PIFs negatively regulate phyB levels.

INTRODUCTION

Plants are informed of the time of the day and their place of growth by a collection of photoreceptors that detect changing intensity, quality, and direction of light in the environment. Among these, only the phytochrome (phy) family members are sensitive to red (R) and far-red (FR) light. Phytochromes exist as dimers that upon R exposure change their conformation from the inactive (Pr) to the active (Pfr) form; the latter translocates into nuclei to initiate a signaling cascade leading to photomorphogenic responses (Neff et al., 2000; Bae and Choi, 2008; Fankhauser and Chen, 2008). Based on their relative stability upon light treatment, phytochrome family members are broadly classified into two groups. The labile phytochrome, type I, contains only one family member, phyA, which is rapidly degraded during seedling deetiolation. This phytochrome plays a major role in a plant's transition from heterotrophic to phototrophic growth (Neff et al., 2000; Bae and Choi, 2008). On the other hand, type II phytochromes, phyB, C, D, and E, are relatively stable and slowly degraded upon irradiation with R (Sharrock and Clack, 2002). These phytochromes mediate a large number of physiological and molecular responses, from

seed germination and shade avoidance to flowering (Smith, 2000).

PhyA instability in the light is a mechanism of photoreceptor desensitization linked to signal termination. Previous work has shown that the phyA PAS domain interacts with the WD40 domain of CONSTITUTIVE PHOTOMORPHOGENIC1 (COP1) and that COP1 acts as an E3 ligase for the photoreceptor (Seo et al., 2004). Consistent with these observations, phyA and COP1 colocalize in nuclear bodies, and the phyA destruction rate is decreased in *cop1* mutant alleles and by expression of a dominant-negative COP1 RING motif mutant (Seo et al., 2004). COP1 activity toward its target proteins can be modulated by factors that interact with this E3 ligase. Indeed, SPA1, which binds to the coiled-coil domain of COP1, has been shown to regulate COP1-mediated ubiquitination of phyA, LAF1, and HY5 (Saijo et al., 2003, 2008; Seo et al., 2003, 2004). These observations raise the possibility that factors that interact with COP1 substrates may also affect their ubiquitination.

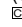
Like phyA, the stable phytochromes (e.g., phyB) are also converted to the active Pfr form by R and can be reverted to the inactive Pr form by darkness or FR. Although FR and darkness can desensitize phyB, the question arises whether the nuclear, activated Pfr form also undergoes turnover during light signaling and how this critical step in R light signaling is regulated. Even at high R light fluences, only 50 to 60% of the total phyB is converted into Pfr, which is compartmentalized in nuclei (Chen et al., 2005). Whether the cytosolic and nuclear phyB pools have different turnover rates and are differentially regulated has not been explored.

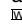
Work done primarily by Quail and colleagues has identified a group of basic helix-loop-helix (bHLH) transcription factors, named phytochrome interacting factors (PIFs), that interact

¹Current address: Department of Plant Science, Seoul National University, Seoul 151-921, Korea.

²Address correspondence to chua@mail.rockefeller.edu.

The author responsible for distribution of materials integral to the findings presented in this article in accordance with the policy described in the Instructions for Authors (www.plantcell.org) is: Nam-Hai Chua (chua@mail.rockefeller.edu).

Some figures in this article are displayed in color online but in black and white in the print edition.

Online version contains Web-only data.

www.plantcell.org/cgi/doi/10.1105/tpc.109.072520

with phytochromes (Castillon et al., 2007; Monte et al., 2007). PIFs accumulate in darkness and inhibit photomorphogenesis by promoting transcription of genes that positively regulate cell elongation (Martínez-García et al., 2000; de Lucas et al., 2008; Feng et al., 2008; Leivar et al., 2008a). Detailed biochemical analysis has showed that, upon light exposure, PIF1, 3, 4, 5, 6, and 7 can interact with phytochrome via an active phytochrome binding motif (APB) (Huq et al., 2004; Khanna et al., 2004; Leivar et al., 2008a). Binding to phyB targets PIF1, 3, 4, and 5 for degradation by 26S proteasomes (Castillon et al., 2007; Monte et al., 2007; Henriques et al., 2009). There is an inverse relationship between phyB levels and PIF levels; *pif* mutants accumulate higher phyB levels, whereas PIF overexpressors have reduced phyB levels (Khanna et al., 2007; Al-Sady et al., 2008; Leivar et al., 2008a). Because PIFs are localized in nuclei, these results suggest that the nuclear phyB pool, presumably consisting of phyB Pfr, is unstable and regulated by PIFs. The E3 ligase(s) responsible for phyB instability has not yet been identified, and the mechanism of action of PIFs is also unknown.

Here, we identify COP1 as the E3 ligase for not only phyB but also other members (phyC-E) of the stable phytochrome family. We found that PIFs enhance phyB ubiquitination by COP1 in vitro and the phyB interacting motif (APB) is needed for this stimulation. Furthermore, we show that, in R light, nuclear and cytoplasmic phyB pools are differentially regulated, since PIFs promote COP1-mediated ubiquitination of only nuclear phyB. Taken together, our results provide a mechanism for the desensitization of type II phytochromes and signal termination under R light conditions and uncover the mechanisms by which the abundance of PIFs modulates this key step in light signaling.

RESULTS

Increased phyB and phyD Levels in *cop1* Mutant Alleles

We examined the phenotypes of *cop1* mutant alleles under R light using wild-type (Columbia-0 [Col-0]) and *phyB-9* as controls. In agreement with previous observations (McNellis et al., 1996), *cop1* mutant alleles (*cop1-4* and *cop1-6*) were hypersensitive to R with shorter hypocotyls and larger cotyledons compared with wild-type seedlings (Figure 1A). Under the same conditions, the phenotype of the *phyB-9 cop1-4* double mutant (Yu et al., 2008) shows slight hyposensitivity to R light compared with *cop1-4* (see Supplemental Figure 1 online).

The R hypersensitivity of *cop1* mutants could be due to many factors, such as reduced expression of negative regulatory components and/or increased expression of positive signal transducers, including photoreceptors. To address this, we first analyzed expression levels of two phytochromes: phyB and phyD implicated in R signaling. As members of the stable phytochrome family, phyB and phyD are known to turn over in R but at a much slower rate compared with phyA (Sharrock and Clack, 2002). We confirmed these previous observations (see Supplemental Figure 2 online) and also showed that *cop1* mutant alleles accumulated higher levels of these photoreceptors compared with the wild type (Figure 1A). In the wild type, both phyB and phyD were moderately unstable and degraded by 26S

proteasomes after 24 h of R light, as demonstrated by their increased levels in the presence of MG132 (Figure 1B). By contrast, phyB and phyD appeared to be stable in *cop1* mutants treated with R, and their levels were not affected by MG132, suggesting reduced degradation (Figure 1B). Although in seedlings germinated in darkness, *phyB* or *phyD* mRNA levels were higher in *cop1-4* compared with the wild type, there were no significant differences of these mRNA levels under R treatment (see Supplemental Figure 3 online), where pronounced differences in phyB levels between *cop1-4* and the wild type were observed (Figure 1B).

phyB Interacts with COP1 in Vitro and in Vivo

Because COP1 is an E3 ligase (Saijo et al., 2003; Seo et al., 2003), the stability of phyB in *cop1* mutant alleles suggested that the photoreceptor could be a substrate. We performed in vitro pull-down assays to test for direct interaction between PhyB and COP1. Whereas the N-terminal (PhyB-N, amino acids 1 to 640) region of PhyB strongly interacted with COP1, weak binding was detected with the C-terminal (PhyB-C, amino acids 640 to 1172) region (cf. Figures 1C and 7B). The binding of the PhyB N-terminal fragment to COP1 was not as strong as that of HFR1, which was used as a positive control. Neither maltose binding protein (MBP) nor glutathione S-transferase (GST) interacted with any of the proteins tested. Further deletion analysis showed the WD40 domain (amino acids 216 to 675) of COP1 was responsible for the binding (see Supplemental Figure 4 online). The direct in vitro interaction between phyB and COP1 could be recapitulated in vivo using transgenic plants expressing COP1-6Myc fusion protein (Figure 1D).

COP1 Is an E3 Ligase for PhyB

The direct interaction between COP1 and PhyB prompted us to perform in vitro ubiquitination assays to test whether PhyB would be a COP1 substrate. Figure 2A shows that PhyB-N but not PhyB-C could be polyubiquitinated by COP1. This result indicates that COP1 is an E3 ligase for PhyB and that a strong, direct interaction is necessary for polyubiquitination. In plants, phyB can exist in two forms, Pr and Pfr, depending on the ambient light condition. Accordingly, we reconstituted phyB-N using the cyanobacterial phycocyanobilin as a chromophore (Ni et al., 1999), and the generated Pr and Pfr forms of phyB-N were used as substrates for in vitro ubiquitination. Figure 2B shows that the Pfr form rather than the Pr form of phyB was preferentially polyubiquitinated by COP1 after 1 h of incubation in vitro. Upon longer incubation, however, polyubiquitination of the Pr form was also seen. These results show that COP1 can ubiquitinate both forms of phyB-N but with different efficiencies.

If phyB is targeted by COP1 E3 ligase in vivo, we should be able to manipulate phyB levels by changing endogenous COP1 activity. To this end, we expressed COP1-6Myc or DN-COP1-6Myc in transgenic plants using an inducible system. Figures 2C and 2D show that phyB and phyD expression levels were decreased by induced wild-type COP1 expression but increased when the expression of a dominant-negative COP1 RING motif mutant was induced (Seo et al., 2004). These results provide

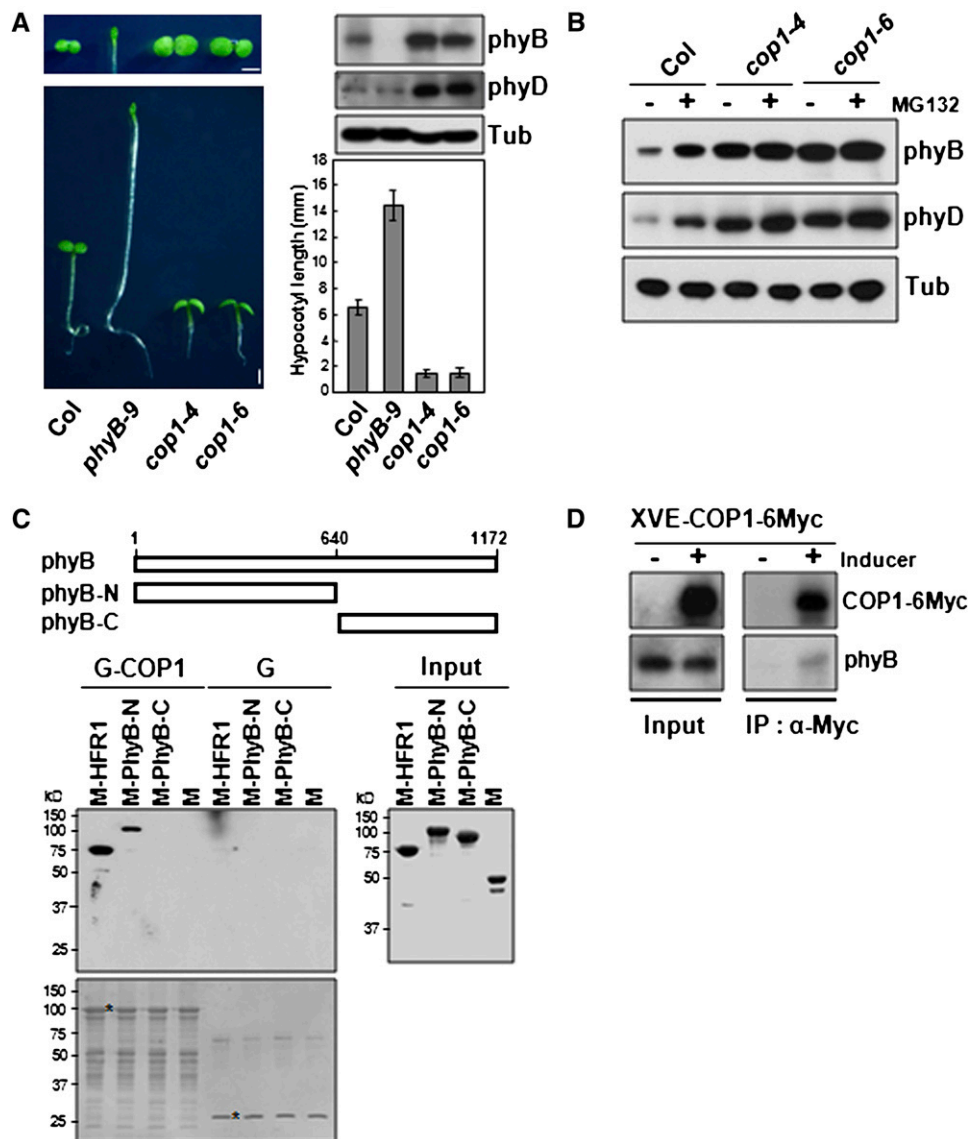


Figure 1. phyB Interacts with COP1.

(A) Phenotypes of the wild type (Col), *phyB-9*, *cop1-4*, and *cop1-6* under R light. Hypocotyls (bottom left panel) and cotyledons (top left panel) after R light treatment for 4 d. Bar = 1 mm. Bottom right panel: Average hypocotyl length \pm SD ($n > 40$) for each genotype. Top right panel: phyB and phyD protein levels using anti-phyB (BA2) and anti-phyD antibodies, respectively. Tubulin (Tub) was measured as a loading control.

(B) Immunoblots showing phyB and phyD protein accumulation in *cop1* mutants under R light. Four-day-old etiolated wild-type (Col) seedlings were treated with or without MG132 (25 μ M) and exposed to R light for 24 h.

(C) In vitro pull-down assay showing interaction between PhyB-N and COP1. Top panel: Schematic diagrams of full-length PhyB, PhyB-N-, and PhyB-C-terminal region. Membrane staining (bottom blot) after pull-down assay was used to monitor amounts of bait proteins. Asterisks indicate the bait proteins GST-COP1 (G-COP1) or GST (G). Input, purified MBP-fused target proteins used in pull-down assays. HFR1 was used as a positive control. M, MBP

(D) In vivo pull-down assay showing interaction between phyB and COP1. Transgenic seedlings (XVE-COP1-6Myc) were incubated in the presence or absence of inducer to stimulate the expression of Myc-tagged COP1. Protein extracts (shown in Input lanes) were immunoprecipitated with anti-Myc (IP: α -Myc), and blots were probed with anti-Myc and anti-PhyB.

[See online article for color version of this figure.]

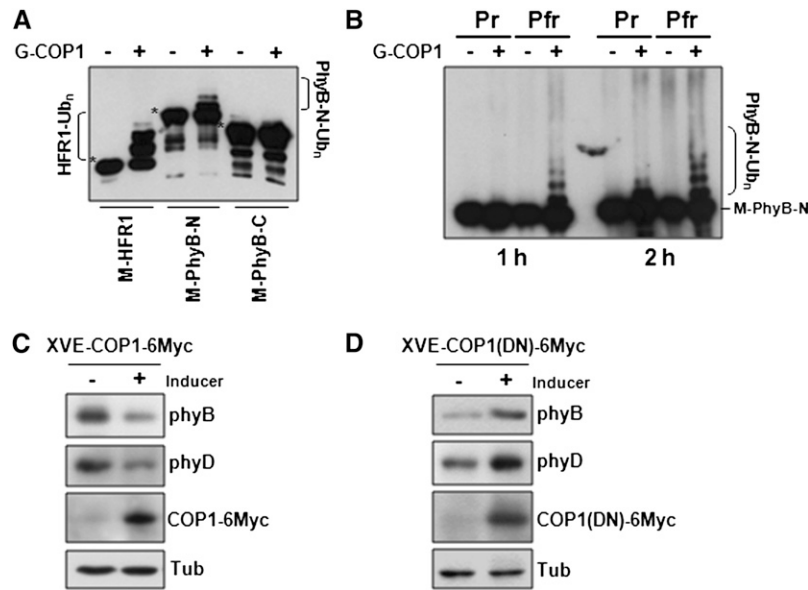


Figure 2. In Vitro Ubiquitination of PhyB by COP1 E3 Ligase.

(A) COP1-mediated ubiquitination of PhyB N-terminal domain. MBP fusions with HFR1 or the N- or C- terminal domains of PhyB were incubated with E1 ubiquitin activating enzyme and E2 ubiquitin conjugating enzyme in the presence or absence of GST-COP1 (G-COP1). Immunoblots of the reactions were probed with anti-MBP. Asterisks indicate the original size of M-HFR1, M-PhyB-N, and M-PhyB-C.

(B) COP1 preferentially ubiquitinates Pfr of phyB-N. MBP-phyB-N reconstituted with the chromophore PCB was used as substrate in in vitro ubiquitination assays. In vitro ubiquitination assay was performed at 30°C for 1 h or 2 h with Pfr and Pr forms of MBP-fused phyB-N (M-phyB-N).

(C) Immunoblots showing decreased phyB and phyD levels in transgenic plants after induction of COP1 expression under R light.

(D) Immunoblots showing increased phyB and phyD levels after inducing the expression of a dominant-negative mutant COP1(DN) under R light. In **(C)** and **(D)**, phyB, phyD, and COP1 levels were detected by anti-phyB (BA2), anti-phyD, and anti-Myc antibodies, respectively. Tubulin (Tub) was detected as a loading control.

evidence that COP1 E3 ligase directly regulates phyB and phyD levels in vivo.

Nuclear Pfr phyB Is Unstable

In darkness (D), phyB is localized in the cytosol, but upon R treatment, the activated photoreceptor (presumably phyB Pfr) translocates into nuclei (Yamaguchi et al., 1999; Kircher et al., 2002; Chen et al., 2003). To determine how nuclear translocation affects phyB, we compared phyB levels in etiolated seedlings and seedlings exposed to 24 h R. Figure 3A shows that phyB was relatively stable in darkness when the inactive photoreceptor was cytosolic but was degraded by 26S proteasomes upon R irradiation when the photoreceptor had translocated into nuclei. The half-life of phyB in darkness was longer than under R light (see Supplemental Figure 5 online); in fact, in darkness phyB levels remained unchanged for 24 h. These observations suggest that phyB degradation in R light is largely a nuclear event. To test this hypothesis, we examined the stability of an N-terminal fragment of phyB appended with green fluorescent protein (GFP), β -glucuronidase (GUS), and a nuclear localization signal (NGG-NLS). This fusion protein, which is constitutively nuclear localized, has been shown to complement a *phyB* null mutation (Matsushita et al., 2003). Figure 3B shows that in contrast with phyB, NGG-NLS was unstable both in D as well as after 24 h R

treatment, but its level could be greatly increased with MG132, indicating that the nuclear-targeted NGG-NLS was rapidly degraded under both conditions. By contrast, CG (phyB C-terminal-GFP) levels were relatively high in D and R, and MG132 had only a small effect. Coimmunoprecipitation experiments demonstrated that NGG-NLS but not CG interacted with COP1 in vivo (see Supplemental Figure 6 online).

We next determined the half-life of different phyB derivatives using transgenic plants expressing BG (phyB-GFP), NGG-NLS, and CG (Matsushita et al., 2003) treated with cycloheximide to block new protein synthesis. Under the experimental conditions used, the half-life of phyB in the wild type (Col) was ~8 h under R (Figure 5A, Col), and the BG decay rate or pattern was comparable to that of phyB (Figure 3C). By contrast, the NGG-NLS decay rate was remarkably faster and the protein was no longer detectable after 2 h (Figure 3C). Control experiments showed no change in CG levels for 24 h (Figure 3C). The NGG-NLS fast decay pattern is reminiscent of that displayed by HFR1, LAF1, HY5, and BIT1, which are nuclear transcription factors also targeted by COP1 (Osterlund et al., 2000; Jang et al., 2005, 2007; Hong et al., 2008).

The slower decay kinetics of BG or phyB (Figures 3C and 5A) compared with NGG-NLS in R was surprising. One possible explanation could be that in contrast with NGG-NLS, a fraction of phyB was translocated into the nucleus in R and degradation

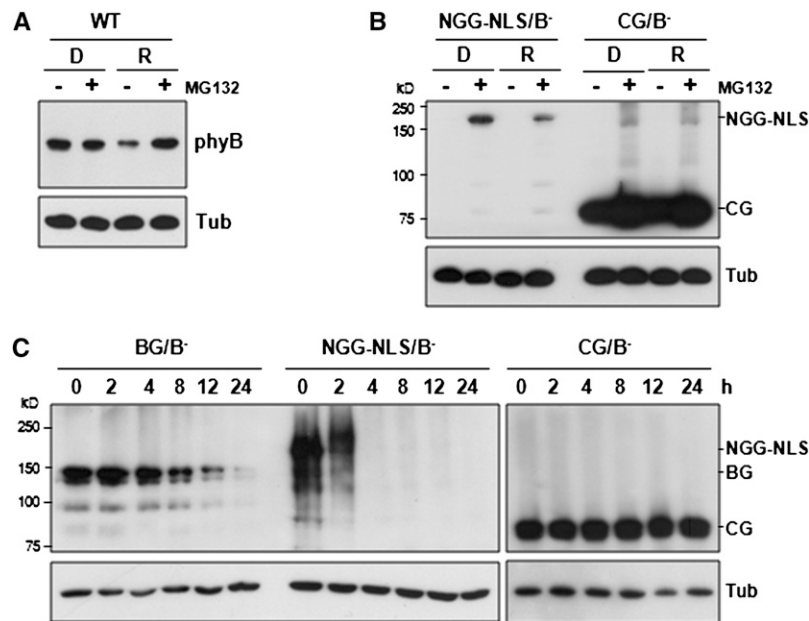


Figure 3. N-terminal Fragment of phyB Is Unstable in Transgenic Plants.

(A) phyB levels in wild-type (WT) *Arabidopsis* seedlings (*Ler*) under D and R for 24 h in the presence or absence of MG132.

(B) Protein immunoblot analysis of transgenic *Arabidopsis* seedlings (NGG-NLS/B⁻ and CG/B⁻) under D and R for 24 h in the presence or absence of MG132. NGG-NLS and CG levels were detected by anti-GFP antibody. Tubulin (Tub) was detected as a loading control.

(C) Posttranslational decay experiment showing fast decay rate of NGG-NLS under R light. Blots were probed with anti-GFP antibody.

occurred only in the nuclear compartment. The relative stability of the remaining cytosolic phyB pool could account for the dampened decay rate of the total phyB population. To address this issue directly, we performed cell fractionation experiments using etiolated seedlings as well as seedlings exposed to 6 and 24 h of R (R6 and R24). Figure 4A shows results confirming the purity of the two cell fractions as evidenced by the preferential

distribution of RNA polymerase II (Pol II) and α -tubulin (Tub), which were used as nuclear and soluble (presumably cytosolic) markers, respectively. In the same samples, phyB was clearly present in the soluble fractions in D, R6, and R24 but was not detectable in the nuclear fractions (Figure 4A). Addition of MG132 increased phyB levels in the nuclear fractions of R24 (R24+MG132), indicating that phyB was translocated into the

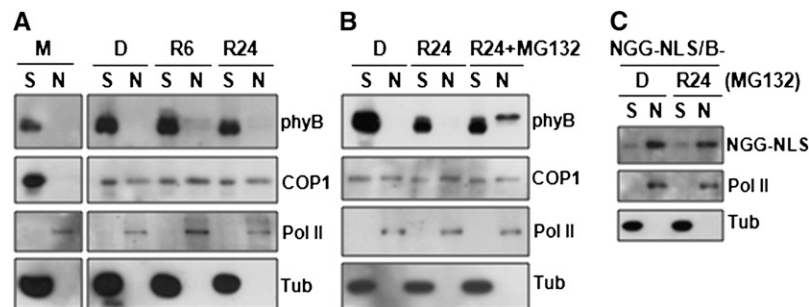


Figure 4. phyB Is Unstable in Nuclei under R Light.

(A) Nuclear phyB is unstable under R light. Two-week old wild-type (Col-0) *Arabidopsis* plants grown under long days (16 h light/8 h dark) (M) as well as 4-d-old etiolated seedlings that were kept in the dark (D) or transferred to R light for 6 or 24 h (R6 and R24, respectively) were fractionated.

(B) Nuclear phyB levels can be increased by MG132 (25 μ M) under R light.

(C) NGG-NLS is localized in nuclei under R light. Four-day-old etiolated seedlings (NGG-NLS/B⁻) were treated with MG132 (25 μ M) and then kept in D or exposed to R light (10 μ mol m⁻² s⁻¹) for 24 h.

In **(A)** to **(C)**, samples were fractionated as soluble (S) and nucleus (N). Pol II and tubulin were used as the marker proteins for nuclear and cytosol fractions, respectively, as well as the loading controls.

nucleus and degraded in R (Figure 4B). Note that the electrophoretic mobility of nuclear phyB (R24+MG132) was slower than that of cytosolic phyB. This was likely a consequence of the increased salt concentration in the nuclear fraction. We next investigated NGG-NLS, which is constitutively localized in the nucleus. Figure 4C shows that, after MG132 treatment, the majority of NGG-NLS accumulated in nuclei in both D and R24, confirming the reliability of these cell fractionation experiments.

Because phyB is a substrate of COP1, we investigated the distribution of COP1 in the same fractions using a specific COP1 monoclonal antibody (see Supplemental Figure 7A online). COP1 was found in both the soluble as well as the nuclear fraction, and its distribution was not altered by R treatment (Figures 4A and 4B). Moreover, we found that COP1 was mostly in the soluble fraction in mature *Arabidopsis thaliana* plants (Figure 4A, M). Our results suggest that COP1 may be active only in the nucleus and at early stages of seedling development.

***pif* Mutants Accumulate Higher phyB Levels Compared with the Wild Type**

Since phyB photoactivation initiates R signaling, it is reasonable to assume that photoreceptor desensitization by protein destruction may be subject to multiple regulations. Such regulatory factors are expected to interact with either phyB or COP1. PIFs are members of the bHLH family first identified by their binding to activated phyB through their APB sequences (Ni et al., 1999; Khanna et al., 2004). These nuclear factors negatively regulate phyB levels, which increase in *pif* mutants but decrease in PIF overexpressors (Khanna et al., 2007; Al-Sady et al., 2008; Leivar et al., 2008a). However, it is not known if this effect is direct or indirect, and the mechanism of PIF action remains obscure.

We measured phyB turnover kinetics in the wild type and *pif* mutants in the absence of new protein synthesis. We found that the half-life of phyB was ~8 h in the wild type (Col) but was prolonged to ~24 h in *pif* single mutants and further increased to more than 24 h in *pif* double mutants and *cop1-4* (Figure 5A). When analyzed on the same gel blot, *pif3 pif4* and *pif4 pif5* double mutants and *cop1-4* clearly accumulated higher phyB levels compared with the wild type (Figure 5B) confirming previous results (Khanna et al., 2007; Al-Sady et al., 2008; Leivar et al., 2008a). Cell fractionation experiments showed that compared with the wild type, *cop1* and *pif* double mutants accumulated detectable levels of nuclear phyB in the absence MG132 (Figures 5C to 5E), supporting the notion of active nuclear COP1. Note that in these double mutants, nuclear phyB levels were still elevated by MG132 treatment, suggesting that PIF3, 4, and 5, and perhaps other related factors, may act redundantly (Leivar et al., 2008b). Direct comparison of nuclear phyB levels on the same blot showed that nuclear phyB levels were considerably higher in *pif4 pif5* and *cop1-4* (Figure 5F). This phyB population appeared to be less labile, as the effect of MG132 was only moderate.

In addition to confirming the observations about higher phyB levels or delayed phyB decay rate in *pif* mutants and/or the *cop1* mutant (Khanna et al., 2007; Leivar et al., 2008a; Figure 5), our results also show that mostly the nuclear phyB pool is affected by PIFs and/or COP1.

PIFs Facilitate Polyubiquitination of phyB by COP1 E3 Ligase

The effects of PIFs on phyB levels may be direct or indirect. We hypothesized that perhaps binding of PIFs via their APB sequences to phyB may enhance photoreceptor ubiquitination by COP1. This hypothesis is consistent with the report that phyB levels are lower in PIF3 and PIF5 overexpressors (Khanna et al., 2007; Al-Sady et al., 2008). We tested this hypothesis directly by *in vitro* ubiquitination assays. Figures 6A and 6B show that, indeed, PIF5 was able to enhance polyubiquitination of PhyB-N. This stimulatory effect depended on binding of PIF5 to PhyB-N since a noninteracting mutant, mPIF5 (E31A/G37A) (Khanna et al., 2004), was inactive and in fact inhibited the polyubiquitination reaction at all amounts except 50 ng (Figure 6B; see Supplemental Figure 8 online). Unexpectedly, at 50 ng, mPIF5 appeared to stimulate PhyB-N ubiquitination compared with wild-type PIF5. The mechanism of this anomalous result was not further investigated. Similar enhancement of PhyB-N ubiquitination was obtained for PIF3 and PIF4; moreover, we found that the three PIF factors can act synergistically in this reaction (Figure 6A). These results are consistent with the observation that *pif* double mutants accumulate high phyB levels compared with single mutants (Figure 5A).

We wanted to explore the mechanism by which phyB polyubiquitination is increased by PIFs. To this end, we analyzed the effect of PIF on PhyB/COP1 interaction by *in vitro* pull-down assay using PIF5 as a representative of PIFs. Figure 6C shows that PhyB/COP1 interaction was enhanced by increasing amounts of PIF5. This effect of PIF5 was dependent on PIF5/PhyB interaction, since neither the noninteracting mutant mPIF5 (E31A/G37A) nor HFR1, a bHLH protein, had any effect.

We also confirmed that COP1 interacted with PIF3, 4, and 5 (Figure 6D). However, these PIFs were not ubiquitinated by COP1 E3 ligase (Figure 6E), indicating that they are not COP1 substrates. Our result is consistent with previous report (Bauer et al., 2004) showing that COP1 does not affect the light-dependent PIF3 turnover and that other E3 ligases are involved in the proteolysis of PIFs. Taken together, our findings suggest that PIFs are likely required to strengthen PhyB/COP1 interaction so as to enhance PhyB ubiquitination and turnover and this function of PIFs is independent of their transcriptional activity.

COP1 Is an E3 Ligase of Five *Arabidopsis* Phytochromes

We also investigated whether other stable phytochromes are also substrates of COP1. Figure 7A shows that COP1 interacted strongly with the N-terminal regions (PhyC-N, amino acids 1 to 592; PhyD-N, amino acids 1 to 644) of phyC and phyD but weakly with the C-terminal regions of these two phytochromes. In the case of phyE, both the N- (amino acids 1 to 588) and the C-terminal regions (amino acids 589 to 1112) interacted with similar affinity to COP1. *In vitro* assays confirmed that phytochrome regions that strongly bound to COP1 were also polyubiquitinated by the E3 ligase (Figure 7B). Note that ubiquitination of phyE-N and phyE-C by COP1 was not as efficient as that of the others. Our results confirmed that in addition to serving as an E3

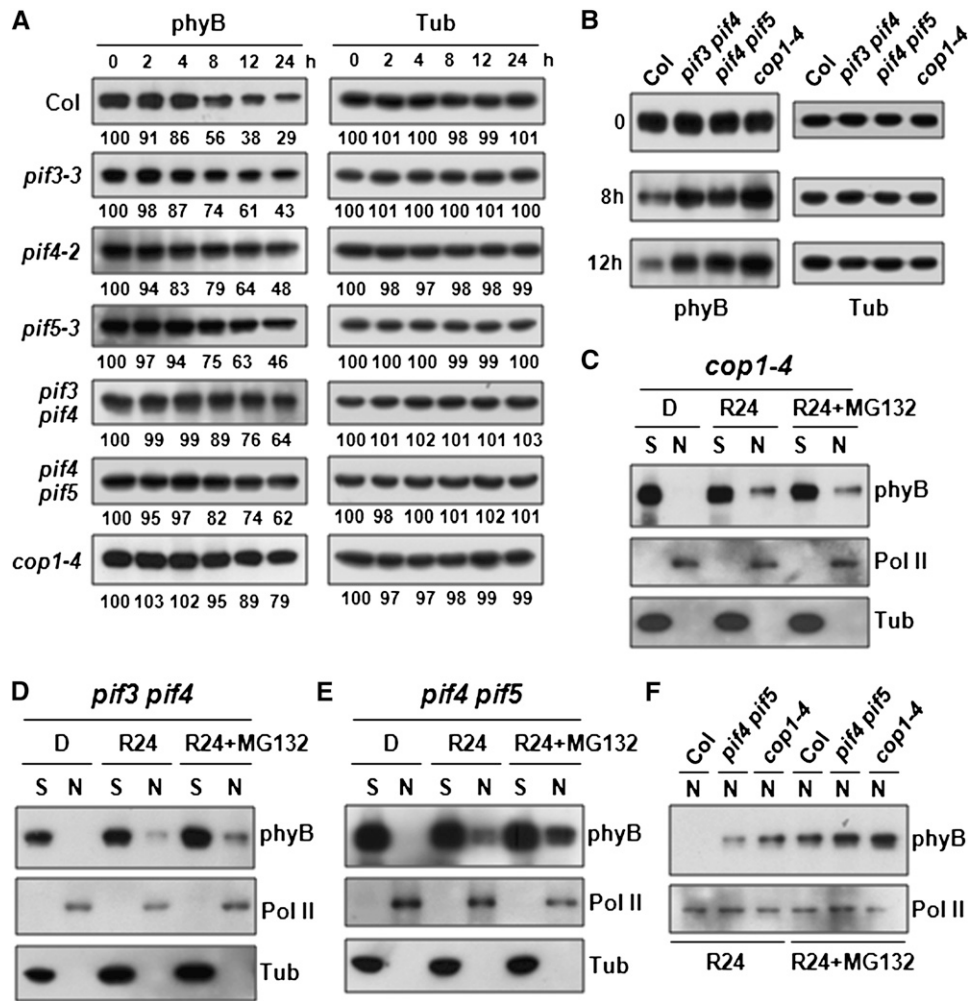


Figure 5. *pif* Mutants Accumulate Higher phyB Levels Compared with the Wild Type.

(A) phyB decay is delayed in *pif* mutants and *cop1-4* under R light.

(B) phyB levels in *pif3 pif4*, *pif4 pif5*, and *cop1-4* compared with the wild type. Samples (0, 8, and 12 h after cycloheximide treatment) were chosen from (A) and analyzed on the same blot.

(C) to (E) Nuclear phyB levels are elevated in *cop1-4* (C), *pif3 pif4* (D), and *pif4 pif5* (E).

(F) Direct comparison of nuclear phyB levels in the wild type (Col), *pif4 pif5*, and *cop1-4*.

In (C) to (F), sample fractionations and antibodies for marker proteins were identical to those of Figures 4A to 4C.

ligase for phyA (Seo et al., 2004; Saijo et al., 2008), COP1 is an E3 ligase for all phytochromes. Furthermore, direct interaction is required for polyubiquitination.

DISCUSSION

Receptor desensitization and turnover of signaling intermediates by proteolysis are important regulatory steps in signal termination (Henriques et al., 2009). Previous works showed that the phyA photoreceptor is targeted by COP1 E3 ligase for ubiquitination and destruction (Seo et al., 2004; Saijo et al., 2008). Here, we extend this observation to phyB and other stable phytochromes and describe regulatory features of this signaling event.

COP1 Is an E3 Ligase for phyB

The observation that phyB levels were high in *cop1* mutant alleles and were not increased upon MG132 treatment (Figure 1) suggested that phyB is targeted by COP1. Here, we present several lines of evidence to support the claim that COP1 is an E3 ligase for phyB in vivo. (1) The PhyB N-terminal region strongly interacts with the WD40 domain of COP1 (Figure 1C; see Supplemental Figure 4 online). (2) Upon reconstitution with phycocyanobilin, the Pfr form of phyB-N is polyubiquitinated by COP1 at a higher efficiency compared with the Pr form (Figure 2B). (3) *cop1* mutant alleles accumulate phyB whose level is not affected by MG132 (Figure 1B). (4) COP1 associates with phyB in vivo (Figure 1D; see Supplemental Figure 6 online). (5) In

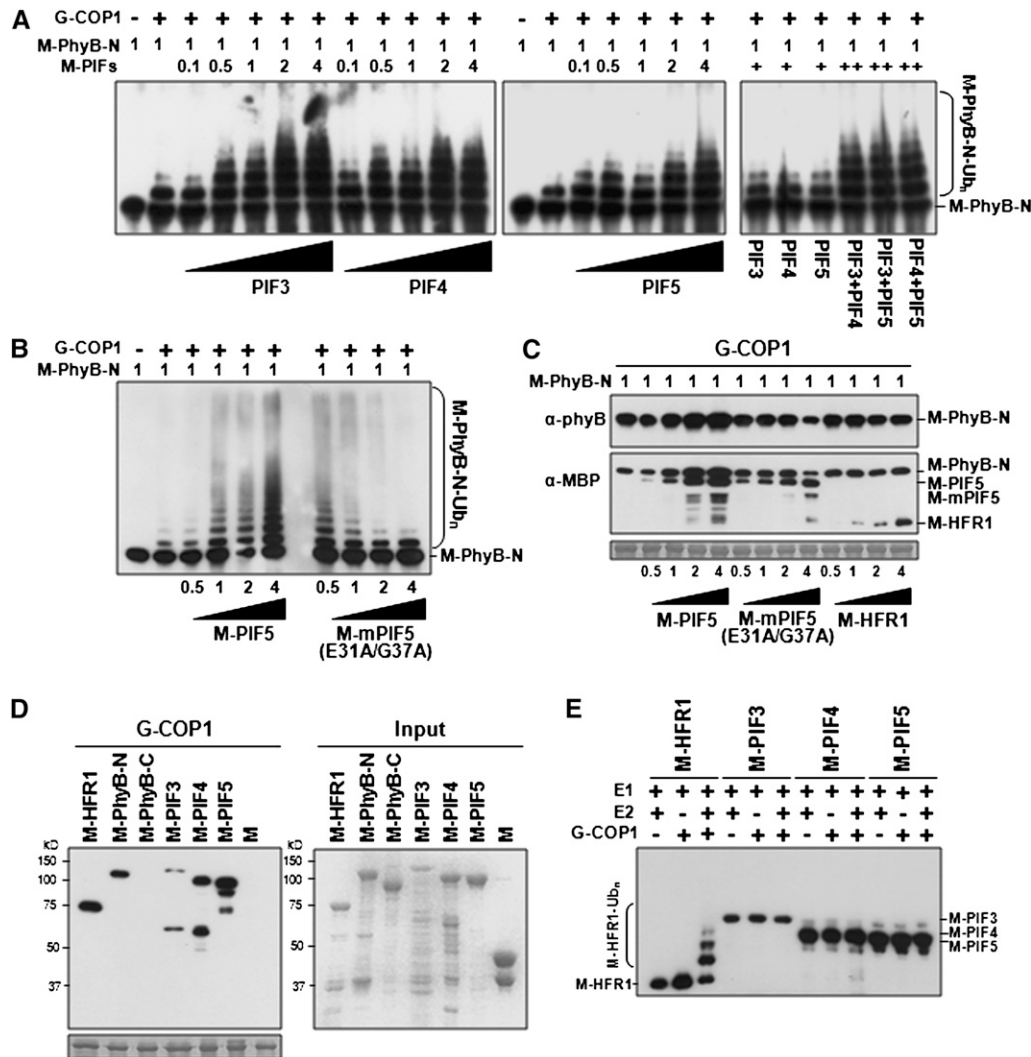


Figure 6. PIFs Facilitate Polyubiquitination of phyB by COP1 E3 Ligase.

(A) Effect of PIFs on PhyB-N ubiquitination by COP1 E3 ligase.

(B) Direct interaction between PIF5 and PhyB enhances phyB ubiquitination by COP1.

(C) In vitro pull-down assay demonstrating that PIF5 promotes PhyB/COP1 interaction.

(D) In vitro pull-down assay showing interaction between PIFs (3, 4, and 5) and COP1. Note that compared with the other proteins, the amount of M-PIF3 used was 5 times less.

(E) In vitro ubiquitination assay of PIF3, 4, and 5 by COP1 E3 ligase.

In (A) and (B), in vitro ubiquitination assays were done with E1 ubiquitin activating enzyme and E2 ubiquitin conjugating enzyme in the presence or absence of GST-COP1 (G-COP1).

In (C) and (D), membrane staining (shown below the immunoblots) after the pull-down assay was used to monitor amounts of bait proteins. Input, purified target proteins used in pull-down assays. Numbers in (A) to (C) indicate the relative amounts of proteins in the reaction, where 1 represents 100 ng M-PhyB-N, M-PIFs, M-mPIF5(E31A/G37A), or M-HFR1. Right panel in (A), PIF3, 4, and 5 were added at 50 ng per reaction.

transgenic experiments, phyB levels are reduced by overexpression of wild-type COP1 but increased by overexpression of a dominant-negative COP1 mutant (Figures 2C and 2D).

Yang et al. (2001) reported an interaction between COP1 and the C-terminal region of PhyB using a yeast two-hybrid system, but the possible interaction between N-terminal region of phyB and COP1 was not investigated. Here, we provide direct evi-

dence demonstrating that the N-terminal region of phyB interacts with COP1 in vitro and in vivo (Figure 1; see Supplemental Figure 6 online), but we also detected weak binding of the C-terminal region by COP1. These results suggest that phyB may harbor two COP1 binding sites in N- and C-terminal regions that have different binding affinities. Consistent with this hypothesis, there appears to be weak interactions between C-terminal

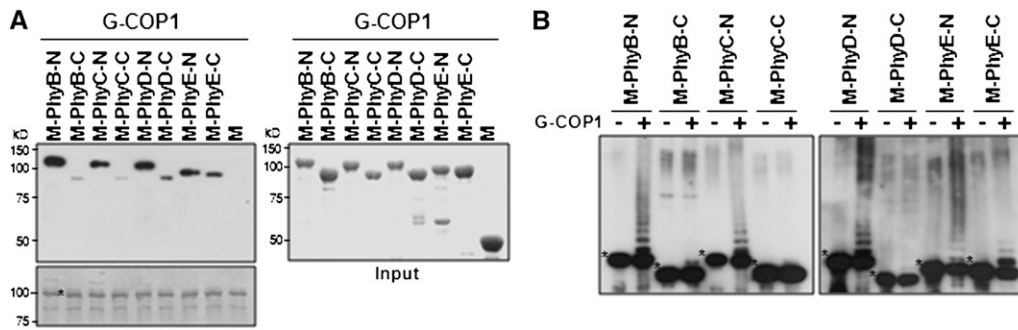


Figure 7. COP1 Ubiquitinates Other Type II Phytochromes through Direct Interaction.

(A) In vitro pull-down assays showing interaction between N- or C-terminal regions of PhyB-E and COP1. Asterisks indicate the original size of N- or C-terminal regions of PhyB-E.

(B) COP1-mediated ubiquitination of N-terminal regions of PhyB-D or N- and C-terminal regions of PhyE. Asterisks indicate original size of the substrates. In vitro ubiquitination assay was done with E1 ubiquitin activating enzyme and E2 ubiquitin conjugating enzyme in the presence or absence of GST-COP1 (G-COP1).

regions of PhyB, PhyD, and PhyE with COP1 (Figure 7A). Furthermore, the expression levels of the C-terminal region of phyB (CG) were slightly increased by MG132 (Figure 3B). However, our result shows that the decay rate of phyB N-terminal fragment (NGG-NLS) is much faster than that of the phyB C-terminal fragment (CG) (Figure 3C). This result is reminiscent of that seen with HFR1 (Jang et al., 2005) in which the deletion mutant HFR1 (Δ N), which has a lower COP1 affinity binding, is considerably more stable than full-length HFR1.

phyB Is Likely Ubiquitinated and Degraded in Nuclei

Upon treatment with R even at high fluences only a fraction of phyB is converted into the Pfr form, which is translocated into nuclei. This raises the possibility that phyB pools in the cytosolic and nuclear compartments may be differentially regulated. We addressed this issue by determining full-length phyB levels in soluble (presumably cytosolic) and nuclear fractions. In addition, we investigated the turnover rate of phyB N- and C-terminal deletion mutants that contain NLS sequences.

Both in darkness and R, phyB appeared stable in the soluble fraction, whereas phyB turnover occurred predominantly in the nuclear fraction. In agreement with this, MG132 had no significant effect on phyB levels in the dark, when the photoreceptor remained cytosolic. By contrast, in R-treated seedlings when a fraction (Pfr form) of phyB becomes nuclear localized, the nuclear phyB pool was detectable only when degradation was arrested by the proteasomal inhibitor MG132 (Figures 4A and 4B). We determined that in the absence of new protein synthesis, phyB levels decreased \sim 70% after 24 h R treatment, suggesting that 30% of the total phyB remains soluble, presumably in the cytosol (Figure 5A). Chen et al. (2003) reported a similar effect in seedlings grown for 4 d in high fluence R, in which only \sim 50% of phyB-GFP was converted into the Pfr form and localized to nuclei. Our results explain why although nuclear phyB is unstable, this photoreceptor has been hitherto considered as a stable phytochrome because its overall decay rate is dampened by the stable cytosolic pool.

Because the N-terminal region of phyB interacts with COP1 and is polyubiquitinated by this E3 ligase (Figures 1 and 2), we compared phyB levels in *phyB* mutants expressing constructs encoding phyB full-length (BG), a functional phyB N-terminal region that is constitutively nuclear (NGG-NLS) or the phyB C-terminal region (CG), including the native NLS motif of phyB (Matsushita et al., 2003). Although both NGG-NLS and CG were found to accumulate in nuclei, NGG-NLS was detected only after MG132 treatment both in darkness and R light (Figure 3B). The instability of NGG-NLS in darkness is likely due to its constitutive nuclear localization as opposed to the R light-triggered nuclear localization of BG (Figure 3C). This result indicating that the Pr form of NGG-NLS can be degraded in the nucleus is consistent with the in vitro observation that the Pr form of phyB-N can also be ubiquitinated by COP1, albeit with reduced efficiency (Figure 2B). Consistent with its instability, the half-life of NGG-NLS is $<$ 2 h (Figure 3C), comparable to those of light-related transcription factors, HY5, HFR1, LAF1, and BIT1, which are also COP1 targets (Osterlund et al., 2000; Jang et al., 2005, 2007; Hong et al., 2008). By contrast, the CG protein, which does not bind to COP1, is very stable both in darkness and under R, notwithstanding its nuclear localization.

COP1 has been reported to localize in nuclei in darkness but migrate to the cytosol upon light exposure (von Arnim and Deng, 1994). It has been proposed that light would promote nuclear exclusion of the E3 ligase thereby allowing accumulation of COP1 targets, such as HY5, leading to the onset of photomorphogenic responses (Osterlund et al., 2000; Saijo et al., 2003). Using a specific monoclonal antibody (see Supplemental Figure 7A online), we monitored COP1 levels in cell fractions prepared from etiolated seedlings or seedlings exposed to R. Surprisingly, we found that COP1 accumulates both in the soluble and nuclear fractions independently of the light treatment (Figures 4A and 4B). These results are not consistent with the view of light-triggered nuclear exit of COP1 during deetiolation. Moreover, under these experimental conditions, COP1 appears to be stable in both compartments, although we had previously shown self-ubiquitination activity in vitro (Seo et al., 2003). Future analysis of

COP1 self-ubiquitination *in vivo* would be necessary to address this issue fully.

Our results show that nuclear turnover of phyB depends on COP1 interaction, whereas the phyB cytosolic pool remains mostly stable. Consistent with these findings, nuclear phyB levels are elevated in *cop1* mutants and insensitive to MG132 treatment (Figures 1B, 5C, and 5F). The findings that phyB and COP1 could potentially also interact in the cytosol and that the Pr form of phyB-N can be modified by COP1 raise the question about the mechanisms that ensure phyB stability in the cytosol. One possibility is that the cytosolic phyB Pr form is also modified by COP1 but the ubiquitinated phyB is rapidly deubiquitinated. Alternatively, cytosolic phyB Pr may bind to one or more unknown proteins that prevent its ubiquitination. Also, photoconversion of phyB Pr into Pfr might expose the N-terminal COP1-interacting region and thus permit enhanced binding of COP1 and subsequent ubiquitination. Finally, photoconversion of phyB combined with the presence of PIF transcription factors in the nuclear compartment could enhance COP1's ability to bind and ubiquitinate the photoreceptor, an event that would not occur in the cytosol, where the PIFs do not localize. Indeed, Chen et al. (2005) reported a conformational change of phyB upon nuclear translocation that results in an open structure allowing unmasking of the NLS signal and possibly the interaction with other proteins, such as COP1.

PIFs Enhance phyB Polyubiquitination by COP1

Previous results with *pif* mutants and PIF overexpressors have shown that, although *phyB* transcript levels remain unchanged, phyB protein levels are negatively correlated with PIF levels, suggesting that these bHLH factors act as negative regulators of the photoreceptor at the posttranslational level (Khanna et al., 2007; Al-Sady et al., 2008; Leivar et al., 2008a). Because PIFs are also nuclear localized, we hypothesized that these factors may regulate ubiquitination of phyB by COP1. Using an *in vitro* assay, we found that PIF3, 4, and 5 enhanced PhyB-N ubiquitination by COP1 (Figures 6A and 6B), and this effect was more pronounced when pairs of PIF (e.g., PIF3+PIF4) were tested (Figure 6A), suggesting that heterodimers might have a synergistic effect. Moreover, we demonstrated that PIFs act directly by binding to phyB-N, since a nonbinding PIF5 mutant (mPIF5) has no stimulatory activity (Figure 6B), suggesting that PIFs (via their APB motif) might increase COP1 affinity toward phyB. Consistent with this notion, the reduced phyB level in PIF3 and PIF5 overexpressors relative to the wild type under R was dependent upon APB activity of these factors (Khanna et al., 2007; Al-Sady et al., 2008).

Further confirmation of the direct role of PIFs in promoting phyB ubiquitination by COP1 came from the analysis of phyB half-life in the wild type, *pif* single and double mutants, and *cop1-4* mutants. In confirmation of previous results (Khanna et al., 2007; Al-Sady et al., 2008; Leivar et al., 2008a), we found that phyB's half-life increased from 8 h in the wild type to 24 h in *pif3-3*, *pif4-2*, and *pif5-3* mutants and further prolonged to more than 24 h in *pif* double mutants (*pif3 pif4* and *pif4 pif5*) and in *cop1-4* (Figure 5). In addition, we showed that in *pif* mutants, nuclear phyB was partially stabilized, providing further support that PIF regulation

of phyB occurs inside nuclei (Figures 5D to 5F). Evidence that PIF proteins act redundantly came from the finding that nuclear phyB levels were slightly increased by MG132 in *pif3 pif4* and *pif4 pif5* double mutants (Leivar et al., 2008b; Figures 5D to 5F). These results support the view that PIFs enhance phyB ubiquitination by COP1 in the nuclei and provide a mechanistic explanation for the inverse relationship seen between PIF and phyB protein levels (Monte et al., 2007; Al-Sady et al., 2008; Henriques et al., 2009). In addition, these findings highlight the importance of PIF proteins in setting nuclear photoreceptor levels.

Our results highlight a new function for PIF proteins, that is, as regulators of COP1 ubiquitination activity toward stable phytochromes. As a major regulator in light signaling, COP1 has been shown to function in concert with regulatory factors like SPA proteins (Laubinger et al., 2004) that are able to modulate its ubiquitination activity toward several transcription factors and even the phyA photoreceptor (Saijo et al., 2003, 2008; Seo et al., 2003). Consistent with the function of SPA proteins *in vivo*, *spa* quadruple mutants displayed a photomorphogenic phenotype in the dark, like *cop1* mutants (Laubinger et al., 2004). Our findings here suggest that in addition to modulating COP1 E3 activity, these signaling factors may function in the selection of ubiquitination targets, providing COP1 with the specificity to regulate FR or R signaling pathways. The finding that *pif1 pif3 pif4 pif5* mutants show a COP1-related phenotype in the dark (Leivar et al., 2008b) further confirms this hypothesis.

The enhancing effect of PIFs on phyB ubiquitination may, on the surface, appear to be similar to the stimulatory effect of SPA1 on PhyA ubiquitination. However, there are major differences between the two that may reflect a different mechanism. First, PIFs but not SPAs are bHLH family transcription factors. Second, SPA1 interacts with the coiled-coil domain of COP1 to increase its E3 ligase activity (Seo et al., 2003), whereas binding of PIFs to both phyB and COP1 is needed to enhance photoreceptor ubiquitination (Figures 6A and 6B; see Supplemental Figure 8 online). So far, it is not known if SPA1 can promote phyA/COP1 interaction.

The stimulatory effect of PIFs on phyB ubiquitination is reminiscent of the modulation of p53 ubiquitination by regulatory factors in animal cells (Sui et al., 2004; Allende-Vega et al., 2007; Kruse and Gu, 2009). The transcription factor Yin Yang 1 (YY1) directly binds to p53 to stimulate polyubiquitination of the latter by Hdm2, and it is thought that YY1 acts by promoting Hdm2-p53 physical interaction (Sui et al., 2004). On the other hand, the transcription factor TAFII250 stabilizes Mdm2, an E3 ligase for p53, through inhibition of its autoubiquitination and thereby indirectly stimulates p53 ubiquitination (Allende-Vega et al., 2007). The role of PIFs in enhancing PhyB ubiquitination by COP1 is reminiscent of the situation in YY1/p53/Hdm2, implying that this mechanism is conserved in eukaryotes.

COP1 Also Targets Other Type II Phytochromes

We found that COP1 could associate with and ubiquitinate PhyC-N, PhyD-N, PhyE-N, and PhyE-C polypeptides (Figures 7A and 7B). Using a commercially available phyD antibody (see Supplemental Figure 7B online), we found that phyD

accumulates in *cop1* mutant alleles independently of proteasome inhibition (Figures 1A and 1B). Our results are consistent with the observation that phyD levels were reduced in PIF5 overexpressors under R (Khanna et al., 2007). Molecular phylogenetic analysis of *Arabidopsis* phytochromes uncovered three divergent phytochrome gene lineages, phyA/C, phyB/D, and phyE (Smith, 2000). The high amino acid sequence identity (>80%) between phyB and phyD, as well as phyD's redundancy in *Arabidopsis* photomorphogenesis, would make phyD the most likely candidate for COP1 and PIFs targeting.

As a type II stable phytochrome, phyB mediates photoresponses ranging from seed germination to shade avoidance and flowering. Here, we provide a molecular mechanism for the termination of R light signal transduction (Figure 8). In the darkness, PIFs accumulate in nuclei where they promote the transcription of elongation genes and repress the onset of

photomorphogenesis (Leivar et al., 2008b). Upon R light exposure, the cytosolic phyB Pr undergoes conformational changes, unmasking its NLS motif to allow for nuclear translocation (Chen et al., 2005). In nuclei, this active Pfr form triggers light responses and promotes PIFs phosphorylation (PIF1, 3, and 5) and PIF degradation by an as yet unknown mechanism. However, upon continued R exposure, signaling by phyB Pfr is terminated by COP1-mediated degradation, which is promoted by PIFs. As PIFs are known to colocalize with phyB in nuclear speckles (Kircher et al., 2002; Bauer et al., 2004), phyB polyubiquitination might occur in these subnuclear structures. Binding of PIFs to both phyB and COP1 might increase the affinity of the photoreceptor for COP1, thereby increasing ubiquitination and degradation. Further understanding of the exact nature of the phyB negative regulation by PIFs will be a challenge for the future.

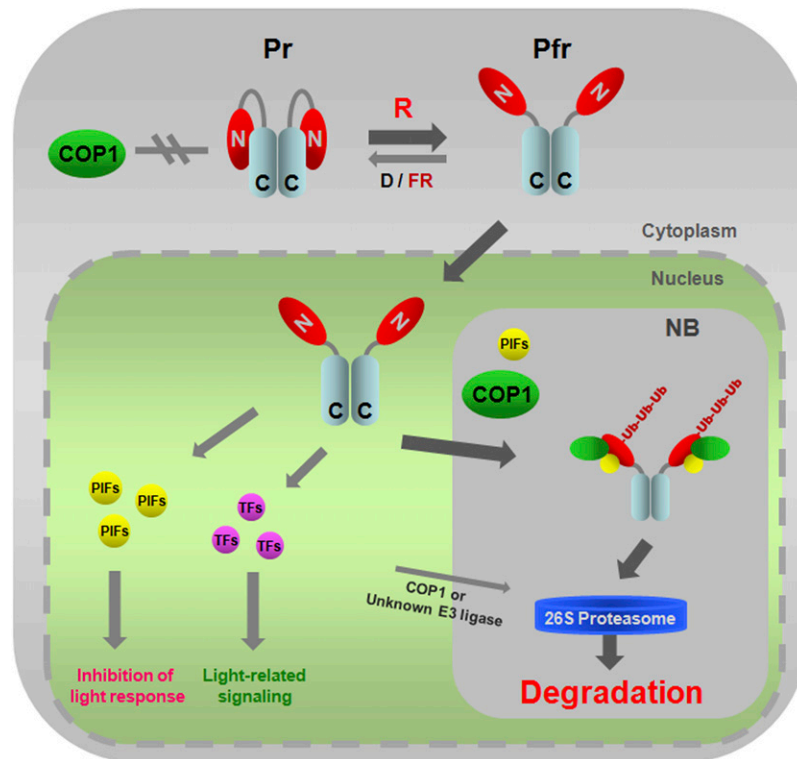


Figure 8. A Model for Light-Dependent Proteasomal Degradation of phyB.

In D or FR light, phyB remains in the cytosol as the inactive Pr form in which both the N-terminal (GAF-PHY domains) and C-terminal regions (PRD) are able to interact (Kircher et al., 1999; Yamaguchi et al., 1999; Chen et al., 2003, 2005). This particular conformation might prevent the association between COP1 and phyB, resulting in a stable phyB that accumulates in the cytosol. However, upon R light exposure, the NLS, located at the C-terminal region of phyB, is exposed due to a light-dependent conformational change (Chen et al., 2005). Therefore, the active Pfr form translocates into nuclei where it triggers signaling by binding to PIFs or other transcription factors (TFs). PIFs may promote phyB polyubiquitination by increasing the binding affinity between phyB and COP1 and thus facilitating phyB degradation by 26S proteasomes. Most probably the phyB-PIFs-COP1 interaction takes place in nuclear bodies (NB), subnuclear structures where COP1 colocalizes with several of its targets (LAF1, HY5, HFR1, and phyA) (Saijo et al., 2003; Seo et al., 2003, 2004; Jang et al., 2005; Yang et al., 2005), since phyB also colocalizes to NB in a PIF3-dependent manner (Bauer et al., 2004). It has been proposed that phyB and PIFs negatively regulate each other (Monte et al., 2007; Al-Sady et al., 2008; Henriques et al., 2009). Although we provide evidence for the PIF-mediated downregulation of phyB levels, the exact mechanism for light-induced and phyB-dependent PIF degradation remains to be characterized.

[See online article for color version of this figure.]

METHODS

Plant Materials

We used the wild type (Col-0 and Landsberg *erecta* [Ler]), *phyB-9* (Reed et al., 1993), *cop1-4*, *cop1-6* (McNellis et al., 1996), *phyB-9 cop1-4* (Yu et al., 2008), *pif3-3* (Monte et al., 2004), *pif4-2* (Leivar et al., 2008a), *pif5-3* (Khanna et al., 2007), *pif3 pif4* (Leivar et al., 2008a), and *pif4 pif5* (Nozue et al., 2007) as plant materials. All mutants were in the Col-0 background.

Transgenic *Arabidopsis thaliana* seedlings of PBG18-5/*phyB-5*, NGGUS-NLS 4-1/*phyB-5*, and CG19-2/*phyB-5* (Matsushita et al., 2003) were designated as BG/B, NGG-NLS/B, and CG/B, respectively. Transgenic *Arabidopsis* seedlings expressing XVE-COP1-6Myc and XVE-COP1(DN)-6Myc were inducible by β -estradiol (Seo et al., 2003, 2004).

Vector Construction and Site-Directed Mutagenesis

Constructs for the production of recombinant GST or MBP fusion proteins were based on plasmids pGEX-4T-1 (GE Healthcare) and pMal-c2 (New England Biolabs), respectively.

The following recombinant proteins were produced in *Escherichia coli*: phyB-N (amino acids 1 to 640), phyB-C (amino acids 640 to 1172), phyC-N (amino acids 1 to 592), phyC-C (amino acids 593 to 1111), phyD-N (amino acids 1 to 644), phyD-C (amino acids 645 to 1164), phyE-N (amino acids 1 to 588), phyE-C (amino acids 589 to 1112), PIF3, PIF4, and PIF5. All relevant cDNA and DNA fragments were amplified by PCR, cloned in pENTR/D vector (Invitrogen), and then transferred into pMBP-DC (Jang et al., 2007) by recombination using the LR Clonase enzyme (Invitrogen). DNA fragments encoding phyD-N and phyE-N were directly inserted into *EcoRI* and *XbaI* restriction sites of pMal-c2.

cDNAs encoding full-length *Arabidopsis* PIF3, PIF4, and PIF5 were amplified by PCR and inserted into *EcoRI* and *XhoI* restriction sites of pGEX-4T-1 to generate G-PIF3, G-PIF4, and G-PIF5. The PIF5 mutant (E31A/G37A) was generated by site-directed mutagenesis using the QuikChange Lightning site-directed mutagenesis kit (Stratagene). Plasmids M-PIF5 and G-PIF5 were used as templates along with appropriate primer sets according to the manufacturer's instructions. All constructs were verified by sequencing. All primer sequences are listed in Supplemental Tables 1 and 2 online.

Plasmids and Preparation of Recombinant Proteins

Plasmids to produce recombinant proteins, MBP-HFR1 (M-HFR1) encoding full-length HFR1, GST-COP1 (G-COP1) encoding full-length COP1, GST-COP1(RC) encoding amino acids 1 to 255 of COP1, and GST-COP1(WD) encoding amino acids 216 to 675 of COP1 were described previously (Jang et al., 2005). Constructs were transformed into *E. coli* BL21 cells and recombinant proteins purified from bacterial extracts after isopropyl- β -D-thiogalactoside induction (Jang et al., 2005).

Light Treatments

For phenotypic analysis shown on Figure 1A and Supplemental Figure 1 online, surface-sterilized wild-type (Col-0) and mutant seeds were vernalized for 4 d at 4°C in darkness, exposed to 1 h of white light, and then transferred to R light ($10 \mu\text{mol m}^{-2} \text{s}^{-1}$) for 4 d at 21°C. Hypocotyl lengths were measured and analyzed using Image J software (<http://rsb.info.nih.gov/ij/>).

Light treatments shown in Figures 1B, 3A, 3B, 4A to 4C, and 5C to 5E were performed with 4-d-old etiolated wild-type (Col-0 or Ler), *pif3 pif4*, *pif4 pif5*, NGG-NLS/B, CG/B seedlings, and/or 4-d-old *cop1* mutants (*cop1-4* and *cop1-6*) seedlings grown in darkness treated with or without MG132 (25 μM) and then kept in darkness (D) or transferred to R light ($10 \mu\text{mol m}^{-2} \text{s}^{-1}$) for 24 h.

For Figures 2C and 2D, transgenic lines carrying XVE-COP1-6Myc or XVE-COP1(DN)-6Myc were treated with or without $10 \mu\text{M}$ β -estradiol to induce COP1-6Myc and COP1(DN)-6Myc expression under R light ($10 \mu\text{mol m}^{-2} \text{s}^{-1}$) for 12 h.

Antibodies for Protein Immunoblotting

Monoclonal antibodies of anti-BA1 and anti-BA2 are specific to the N- and C-terminal domain of phyB, respectively (Matsushita et al., 2003). Mouse anti-COP1 and anti-MBP mAbs were generated by the Monoclonal Antibody Core Facility (Memorial Sloan-Kettering Cancer Center, NY) using purified MBP-COP1 recombinant protein (Jang et al., 2005) as an antigen. Anti-Myc (sc-789), anti-phyD (sc-12710), anti-GST (sc-138), anti-GFP (sc-9996), and anti-Pol II (sc-33754) antibodies were from Santa Cruz Biotechnology and antitubulin antibody was from Sigma-Aldrich (T-9026). Tubulin levels were used as a loading control in all experiments.

In Vitro Pull Down, in Vitro Ubiquitination Assays, and in Vivo Coimmunoprecipitation

Experimental procedures for in vitro pull down, in vitro ubiquitination assays, and in vivo coimmunoprecipitation were described (Jang et al., 2005).

For in vitro pull-down assays, the reaction was done with glutathione sepharose 4B for 2 h. After washing with buffer (50 mM Tris-HCl, pH 7.5, 100 mM NaCl, and 0.6% Triton X-100), pulled-down proteins were separated on 8 to 10% SDS-polyacrylamide gels and detected by protein immunoblotting using anti-MBP or anti-GST antibodies.

For in vitro ubiquitination assays, each reaction mixture (30 μL) contained ~ 100 ng protein substrates, 20 ng rabbit E1 (Boston Biochem), 20 ng human E2 UbcH5b (Boston Biochem), 10 μg His₆-ubiquitin (Sigma-Aldrich), and 200 ng E3 (GST-COP1) and reactions were performed at 30°C for 2 h. Ten microliters of the reaction mixtures were separated on 6% SDS-polyacrylamide gel, and ubiquitinated PhyB-E were detected with anti-MBP for Figures 2A, 2B, 6E, and 7B and anti-phyB (BA1) for Figures 6A and 6B.

The chromophore was attached to M-PhyB-N by adding phycocyanobilin at $10 \mu\text{M}$ final concentration (Ni et al., 1999). The mixture was incubated in darkness for 1 h at 4°C and then treated 10 min of R ($200 \mu\text{mol m}^{-2} \text{s}^{-1}$) or FR ($200 \mu\text{mol m}^{-2} \text{s}^{-1}$) light. In vitro ubiquitination assay was performed at 30°C in darkness.

For in vivo coimmunoprecipitation, 4-d-old etiolated transgenic *Arabidopsis* seedlings [XVE-COP1-6Myc or XVE-COP1(DN)-6Myc] treated with or without β -estradiol ($10 \mu\text{M}$) for 12 h under R light ($10 \mu\text{mol m}^{-2} \text{s}^{-1}$) or 4-d-old etiolated transgenic *Arabidopsis* seedlings (NGG-NLS/B or CG/B) treated with or without MG132 (25 μM) for 12 h under R light ($10 \mu\text{mol m}^{-2} \text{s}^{-1}$) were ground in liquid nitrogen using a precooled mortar and pestle. After extraction of protein in buffer (50 mM Tris-HCl, pH 7.5, 100 mM NaCl, 0.2% Triton X-100, and 1 mM DTT) containing a proteinase inhibitor cocktail (Roche), ~ 1 mg of total protein and 5 μg of anti-Myc polyclonal or anti-COP1 monoclonal antibodies were used for immunoprecipitation reactions. Proteins eluted from protein A/G agarose beads (Roche) were analyzed by immunoblotting using anti-Myc, anti-phyB (BA2), anti-COP1, and anti-GFP antibodies.

Cycloheximide Treatment

Protein decay assays of Figure 5A were done with 4-d-old etiolated seedlings that were transferred to liquid Murashige and Skoog medium containing 100 μM cycloheximide, kept in the dark for 30 min, and then exposed to R light ($10 \mu\text{mol m}^{-2} \text{s}^{-1}$). Samples were harvested as indicated and analyzed by protein immunoblot analysis. Expression levels of phyB and tubulin were measured using the program of Image Gauge V3.12 (Fuji), and the values were normalized to 0 time in all panels.

Protein decay assays of Figure 3C were done with 4-d-old etiolated seedlings (BG/B, NGG-NLS/B, and CG/B) that were treated with MG132 (25 μ M) for 12 h in darkness, washed, and used for decay experiment using cycloheximide as mentioned above. Blots were probed with anti-GFP antibody.

Nuclear Protein Extraction

Nuclear protein extraction was performed using the CellLytic PN extraction kit (Sigma-Aldrich) as described (Abdalla et al., 2009) with minor modifications.

To isolate nuclei, 3 g of tissue from mature plants or 4-d-old etiolated seedlings treated with or without MG132 (25 μ M) for 6 or 24 h under R light (10 μ mol $m^{-2} s^{-1}$) or further kept in darkness for 24 h were ground to a fine powder with liquid nitrogen using a precooled mortar and pestle. Nine milliliters (3 mL/g of tissue) of 1 \times NIB (nuclear isolation buffer from Sigma-Aldrich) was added to ground samples and mixed. The suspension was passed through a filter mesh (100 μ m) and then through miracloth (pore size 22 to 25 μ m) into 50-mL tubes. Organelles including the nuclei were pelleted after centrifugation for 10 min at 1260g, and the supernatant (nuclear depleted soluble fraction) including the cytoplasmic fraction was collected and analyzed as soluble fraction. The pellet was resuspended completely in 0.5 mL of 1 \times NIBA (NIB buffer containing protease inhibitor cocktail), and the organelle membranes were lysed by adding 10% Triton X-100 to a final concentration of 0.3%. For semipure preparation of nuclei, the lysates were applied on top of a 0.8-mL cushion of 1.5 M sucrose with 1 \times NIBA in 1.5-mL tubes. After centrifugation at 12,000g for 10 min, the pellet was collected after removal of upper phase and the sucrose cushion and followed by two times washing with NIBA buffer. The nuclear pellet was resuspended in 100 μ L of nuclear extraction buffer and vortexed for 30 min. Insoluble material was removed by centrifugation at 12,000g for 10 min. The final nuclear protein fraction was transferred into new precooled microcentrifuge tube and stored at $-80^{\circ}C$ until use. An \sim 10-fold nuclear fraction compared with the soluble fraction based on starting material was used for protein immunoblot analyses. Note that all procedures for nuclear protein extraction were performed at $4^{\circ}C$.

RNA Extraction and Quantitative RT-PCR

Total RNA was extracted from *Arabidopsis* seedlings using Qiagen RNeasy plant mini kits (Qiagen). Reverse transcription was performed using the SuperScript III RT kit (Invitrogen). The cDNA was quantified using a SYBR premix Ex Taq (TaKaRa) with gene-specific primers in a Bio-Rad CFX96 real-time system. The oligonucleotides for quantitative PCR were as follows: forward 5'-TCTCGCAGTGAAGTGATTGG-3' and reverse 5'-CCGCTTGTTCAGTCAATA-3' for *phyB* amplification, forward 5'-GTGGTTGTCAACGCATGTTC-3' and reverse 5'-CAAGG-CAGCACGTATTCTCA-3' for *phyD* amplification, and forward 5'-GCA-CCCTGTTCTTACCG-3' and reverse 5'-ACCCTCGTAGATTGGCACA-3' for *ACTIN2* amplification. All reactions were performed in triplicate using three independent RNA samples.

Accession Numbers

Sequence data from this article can be found in the Arabidopsis Genome Initiative or GenBank/EMBL databases under the following accession numbers: *phyB* (At2g18790), *phyC* (At5g35840), *phyD* (At4g16250), *phyE* (At4g18130), *COP1* (At2g32950), *PIF3* (At1g09530), *PIF4* (At2g43010), *PIF5* (At3g59060), and *ACTIN2* (At3g18780).

Supplemental Data

The following materials are available in the online version of this article.

Supplemental Figure 1. Phenotypes of the Wild Type (Col), *phyB-9*, *cop1-4*, and *phyB-9 cop1-4* under R Light.

Supplemental Figure 2. *phyA*, *phyB*, and *phyD* Degradation in R Light.

Supplemental Figure 3. Relative Expression Levels of *phyB* and *phyD* in Col and *cop1-4*.

Supplemental Figure 4. Definition of the COP1 Domain That Binds to PhyB-N.

Supplemental Figure 5. Half-Life of *phyB* in Darkness and under R Light.

Supplemental Figure 6. Coimmunoprecipitation of NGG-NLS with COP1.

Supplemental Figure 7. The Specificity of Monoclonal Anti-COP1 and Polyclonal Anti-*phyD* Antibodies.

Supplemental Figure 8. In Vitro Interaction between PhyB-N and PIFs.

Supplemental Table 1. Primer Sequences for Cloning

Supplemental Table 2. Primer Sequences for Site-Directed Mutagenesis

ACKNOWLEDGMENTS

We thank P.H. Quail for *pif3-3*, *pif4-2*, *pif5-3*, and *pif3 pif4*, C. Fankhauser for *pif4 pif5*, and N.-C. Paek for *phyB-9cop1-4*. We thank S.W. Yang for his help in monoclonal COP1 antibody screening. This work was supported by National Institutes of Health Grant GM44640.

Received October 29, 2009; revised May 7, 2010; accepted June 23, 2010; published July 6, 2010.

REFERENCES

- Abdalla, K.O., Thomson, J.A., and Rafudeen, M.S. (2009). Protocols for nuclei isolation and nuclear protein extraction from the resurrection plant *Xerophyta viscosa* for proteomic studies. *Anal. Biochem.* **384**: 365–367.
- Allende-Vega, N., Saville, M.K., and Meek, D.W. (2007). Transcription factor TAFII250 promotes Mdm2-dependent turnover of p53. *Oncogene* **26**: 4234–4242.
- Al-Sady, B., Kikis, E.A., Monte, E., and Quail, P.H. (2008). Mechanistic duality of transcription factor function in phytochrome signaling. *Proc. Natl. Acad. Sci. USA* **105**: 2232–2237.
- Bae, G., and Choi, G. (2008). Decoding of light signals by plant phytochromes and their interacting proteins. *Annu. Rev. Plant Biol.* **59**: 281–311.
- Bauer, D., Viczián, A., Kircher, S., Nobis, T., Nitschke, R., Kunkel, T., Panigrahi, K.C., Adám, E., Fejes, E., Schäfer, E., and Nagy, F. (2004). Constitutive photomorphogenesis 1 and multiple photoreceptors control degradation of phytochrome interacting factor 3, a transcription factor required for light signaling in *Arabidopsis*. *Plant Cell* **16**: 1433–1445.
- Castillon, A., Shen, H., and Huq, E. (2007). Phytochrome interacting factors: Central players in phytochrome-mediated light signaling networks. *Trends Plant Sci.* **12**: 514–521.
- Chen, M., Schwab, R., and Chory, J. (2003). Characterization of the requirements for localization of phytochrome B to nuclear bodies. *Proc. Natl. Acad. Sci. USA* **100**: 14493–14498.

- Chen, M., Tao, Y., Lim, J., Shaw, A., and Chory, J. (2005). Regulation of phytochrome B nuclear localization through light-dependent unmasking of nuclear-localization signals. *Curr. Biol.* **15**: 637–642.
- de Lucas, M., Daviere, J.M., Rodriguez-Falcon, M., Pontin, M., Iglesias-Pedraz, J.M., Lorrain, S., Fankhauser, C., Blazquez, M.A., Titarenko, E., and Prat, S. (2008). A molecular framework for light and gibberellin control of cell elongation. *Nature* **451**: 480–484.
- Fankhauser, C., and Chen, M. (2008). Transposing phytochrome into the nucleus. *Trends Plant Sci.* **13**: 596–601.
- Feng, S., et al. (2008). Coordinated regulation of *Arabidopsis thaliana* development by light and gibberellins. *Nature* **451**: 475–479.
- Henriques, R., Jang, I.C., and Chua, N.H. (2009). Regulated proteolysis in light-related signaling pathways. *Curr. Opin. Plant Biol.* **12**: 49–56.
- Hong, S.H., Kim, H.J., Ryu, J.S., Choi, H., Jeong, S., Shin, J., Choi, G., and Nam, H.G. (2008). CRY1 inhibits COP1-mediated degradation of BIT1, a MYB transcription factor, to activate blue light-dependent gene expression in *Arabidopsis*. *Plant J.* **55**: 361–371.
- Huq, E., Al-Sady, B., Hudson, M., Kim, C., Apel, K., and Quail, P.H. (2004). Phytochrome-interacting factor 1 is a critical bHLH regulator of chlorophyll biosynthesis. *Science* **305**: 1937–1941.
- Jang, I.C., Yang, J.Y., Seo, H.S., and Chua, N.H. (2005). HFR1 is targeted by COP1 E3 ligase for post-translational proteolysis during phytochrome A signaling. *Genes Dev.* **19**: 593–602.
- Jang, I.C., Yang, S.W., Yang, J.Y., and Chua, N.H. (2007). Independent and interdependent functions of LAF1 and HFR1 in phytochrome A signaling. *Genes Dev.* **21**: 2100–2111.
- Khanna, R., Huq, E., Kikis, E.A., Al-Sady, B., Lanzatella, C., and Quail, P.H. (2004). A novel molecular recognition motif necessary for targeting photoactivated phytochrome signaling to specific basic helix-loop-helix transcription factors. *Plant Cell* **16**: 3033–3044.
- Khanna, R., Shen, Y., Marion, C.M., Tsuchisaka, A., Theologis, A., Schäfer, E., and Quail, P.H. (2007). The basic helix-loop-helix transcription factor PIF5 acts on ethylene biosynthesis and phytochrome signaling by distinct mechanisms. *Plant Cell* **19**: 3915–3929.
- Kircher, S., Gil, P., Kozma-Bognár, L., Fejes, E., Speth, V., Husselein-Muller, T., Bauer, D., Adám, E., Schäfer, E., and Nagy, F. (2002). Nucleocytoplasmic partitioning of the plant photoreceptors phytochrome A, B, C, D, and E is regulated differentially by light and exhibits a diurnal rhythm. *Plant Cell* **14**: 1541–1555.
- Kircher, S., Kozma-Bognár, L., Kim, L., Adam, E., Harter, K., Schäfer, E., and Nagy, F. (1999). Light quality-dependent nuclear import of the plant photoreceptors phytochrome A and B. *Plant Cell* **11**: 1445–1456.
- Kruse, J.P., and Gu, W. (2009). Modes of p53 regulation. *Cell* **137**: 609–622.
- Laubinger, S., Fittinghoff, K., and Hoecker, U. (2004). The SPA quartet: A family of WD-repeat proteins with a central role in suppression of photomorphogenesis in *Arabidopsis*. *Plant Cell* **16**: 2293–2306.
- Leivar, P., Monte, E., Al-Sady, B., Carle, C., Storer, A., Alonso, J.M., Ecker, J.R., and Quail, P.H. (2008a). The *Arabidopsis* phytochrome-interacting factor PIF7, together with PIF3 and PIF4, regulates responses to prolonged red light by modulating phyB levels. *Plant Cell* **20**: 337–352.
- Leivar, P., Monte, E., Oka, Y., Liu, T., Carle, C., Castillon, A., Huq, E., and Quail, P.H. (2008b). Multiple phytochrome-interacting bHLH transcription factors repress premature seedling photomorphogenesis in darkness. *Curr. Biol.* **18**: 1815–1823.
- Martínez-García, J.F., Huq, E., and Quail, P.H. (2000). Direct targeting of light signals to a promoter element-bound transcription factor. *Science* **288**: 859–863.
- Matsushita, T., Mochizuki, N., and Nagatani, A. (2003). Dimers of the N-terminal domain of phytochrome B are functional in the nucleus. *Nature* **424**: 571–574.
- McNellis, T.W., Torii, K.U., and Deng, X.W. (1996). Expression of an N-terminal fragment of COP1 confers a dominant-negative effect on light-regulated seedling development in *Arabidopsis*. *Plant Cell* **8**: 1491–1503.
- Monte, E., Al-Sady, B., Leivar, P., and Quail, P.H. (2007). Out of the dark: How the PIFs are unmasking a dual temporal mechanism of phytochrome signalling. *J. Exp. Bot.* **58**: 3125–3133.
- Monte, E., Tepperman, J.M., Al-Sady, B., Kaczorowski, K.A., Alonso, J.M., Ecker, J.R., Li, X., Zhang, Y.L., and Quail, P.H. (2004). The phytochrome-interacting transcription factor, PIF3, acts early, selectively, and positively in light-induced chloroplast development. *Proc. Natl. Acad. Sci. USA* **101**: 16091–16098.
- Neff, M.M., Fankhauser, C., and Chory, J. (2000). Light: An indicator of time and place. *Genes Dev.* **14**: 257–271.
- Ni, M., Tepperman, J.M., and Quail, P.H. (1999). Binding of phytochrome B to its nuclear signalling partner PIF3 is reversibly induced by light. *Nature* **400**: 781–784.
- Nozue, K., Covington, M.F., Duek, P.D., Lorrain, S., Fankhauser, C., Harmer, S.L., and Maloof, J.N. (2007). Rhythmic growth explained by coincidence between internal and external cues. *Nature* **448**: 358–361.
- Osterlund, M.T., Hardtke, C.S., Wei, N., and Deng, X.W. (2000). Targeted destabilization of HY5 during light-regulated development of *Arabidopsis*. *Nature* **405**: 462–466.
- Reed, J.W., Nagpal, P., Poole, D.S., Furuya, M., and Chory, J. (1993). Mutations in the gene for the red/far-red light receptor phytochrome B alter cell elongation and physiological responses throughout *Arabidopsis* development. *Plant Cell* **5**: 147–157.
- Saijo, Y., Sullivan, J.A., Wang, H., Yang, J., Shen, Y., Rubio, V., Ma, L., Hoecker, U., and Deng, X.W. (2003). The COP1-SPA1 interaction defines a critical step in phytochrome A-mediated regulation of HY5 activity. *Genes Dev.* **17**: 2642–2647.
- Saijo, Y., Zhu, D., Li, J., Rubio, V., Zhou, Z., Shen, Y., Hoecker, U., Wang, H., and Deng, X.W. (2008). *Arabidopsis* COP1/SPA1 complex and FHY1/FHY3 associate with distinct phosphorylated forms of phytochrome A in balancing light signaling. *Mol. Cell* **31**: 607–613.
- Seo, H.S., Watanabe, E., Tokutomi, S., Nagatani, A., and Chua, N.H. (2004). Photoreceptor ubiquitination by COP1 E3 ligase desensitizes phytochrome A signaling. *Genes Dev.* **18**: 617–622.
- Seo, H.S., Yang, J.Y., Ishikawa, M., Bolle, C., Ballesteros, M.L., and Chua, N.H. (2003). LAF1 ubiquitination by COP1 controls photomorphogenesis and is stimulated by SPA1. *Nature* **26**: 995–999.
- Sharrock, R.A., and Clack, T. (2002). Patterns of expression and normalized levels of the five *Arabidopsis* phytochromes. *Plant Physiol.* **130**: 442–456.
- Smith, H. (2000). Phytochromes and light signal perception by plants—an emerging synthesis. *Nature* **407**: 585–591.
- Sui, G., Affar, el B., Shi, Y., Brignone, C., Wall, N.R., Yin, P., Donohoe, M., Luke, M.P., Calvo, D., Grossman, S.R., and Shi, Y. (2004). Yin Yang 1 is a negative regulator of p53. *Cell* **117**: 859–872.
- von Arnim, A.G., and Deng, X.W. (1994). Light inactivation of *Arabidopsis* photomorphogenic repressor COP1 involves a cell-specific regulation of its nucleocytoplasmic partitioning. *Cell* **79**: 1035–1045.
- Yamaguchi, R., Nakamura, M., Mochizuki, N., Kay, S.A., and Nagatani, A. (1999). Light-dependent translocation of a phytochrome B:GFP fusion protein to the nucleus in transgenic *Arabidopsis*. *J. Cell Biol.* **145**: 437–445.
- Yang, H.Q., Tang, R.H., and Cashmore, A.R. (2001). The signaling mechanism of *Arabidopsis* CRY1 involves direct interaction with COP1. *Plant Cell* **13**: 2573–2587.
- Yang, J., Lin, R., Sullivan, J., Hoecker, U., Liu, B., Xu, L., Deng, X.W., and Wang, H. (2005). Light regulates COP1-mediated degradation of HFR1, a transcription factor essential for light signaling in *Arabidopsis*. *Plant Cell* **17**: 804–821.
- Yu, J.W., et al. (2008). COP1 and ELF3 control circadian function and photoperiodic flowering by regulating GI stability. *Mol. Cell* **32**: 617–630.